

# Thiazolides, a New Class of Anti-influenza Molecules Targeting Viral Hemagglutinin at the Post-translational Level<sup>\*S</sup>

Received for publication, June 5, 2009, and in revised form, July 28, 2009. Published, JBC Papers in Press, July 28, 2009, DOI 10.1074/jbc.M109.029470

Jean François Rossignol<sup>†</sup>, Simone La Frazia<sup>§</sup>, Lucia Chiappa<sup>§</sup>, Alessandra Ciucci<sup>§1</sup>, and M. Gabriella Santoro<sup>§2</sup>

From the <sup>†</sup>Department of Medicine, Stanford University School of Medicine, Stanford, California 94305-5187 and the <sup>§</sup>Department of Biology, University of Rome Tor Vergata, 00133 Rome, Italy

The emergence of highly contagious influenza A virus strains, such as the new H1N1 swine influenza, represents a serious threat to global human health. Efforts to control emerging influenza strains focus on surveillance and early diagnosis, as well as development of effective vaccines and novel antiviral drugs. Herein we document the anti-influenza activity of the anti-infective drug nitazoxanide and its active circulating-metabolite tizoxanide and describe a class of second generation thiazolides effective against influenza A virus. Thiazolides inhibit the replication of H1N1 and different other strains of influenza A virus by a novel mechanism: they act at post-translational level by selectively blocking the maturation of the viral hemagglutinin at a stage preceding resistance to endoglycosidase H digestion, thus impairing hemagglutinin intracellular trafficking and insertion into the host plasma membrane, a key step for correct assembly and exit of the virus from the host cell. Targeting the maturation of the viral glycoprotein offers the opportunity to disrupt the production of infectious viral particles attacking the pathogen at a level different from the currently available anti-influenza drugs. The results indicate that thiazolides may represent a new class of antiviral drugs effective against influenza A infection.

Influenza, a highly contagious acute respiratory illness affecting all age groups, is responsible for an average of 36,000 deaths and over 226,000 hospitalizations per year in the United States alone (1). The etiological agent of the disease, the influenza viruses or orthomyxoviruses, are enveloped, negative-stranded RNA viruses classified in three types (A, B, and C), of which the A type is clinically the most important.

The genome of influenza A viruses consists of eight single-stranded RNA segments that encode 11 proteins, including the main surface glycoproteins, hemagglutinin (HA),<sup>3</sup> and neuraminidase (NA), of which 16 HA (H1–H16) and nine NA (NA1–NA9) subtypes have been identified so far (2). Influenza virus

infection involves a series of steps: the virus attaches to host sialylated glycoproteins via the viral hemagglutinin and enters the cell by endocytosis, followed by pH-dependent fusion and release of viral genomic ribonucleoprotein complexes in the cytoplasm. Ribonucleoproteins then translocate to the nucleus where transcription and replication of viral RNA occurs. During the replication cycle some viral proteins translocate to the nucleus for progeny ribonucleoprotein formation, whereas the viral HA, NA, and M2 proteins reach the plasma membrane via the secretory pathway, an event that is essential for viral particle formation and budding from host cells (3). In humans, influenza A virus replicates throughout the respiratory tract, where the viral antigen is found predominantly in the epithelial cells. The typical course of influenza is self-limiting and lasts for about a week; however, clinical responses range from mild disease to fatal viral pneumonia (4, 5). Although the mechanisms underlying the expression of symptoms and the development of secondary complications that may result in respiratory failure are still not well understood, excessive inflammation caused by overabundant production of proinflammatory cytokines and lung inflammatory infiltrates is considered an important factor in disease pathogenesis (6–8).

HA and NA glycoproteins, which are the main targets of the protective immune response, vary continuously as a result of antigenic drift and antigenic shift. Major changes from antigenic shift are caused by the different HA and NA subtypes circulating in birds and other animals that create a reservoir of influenza A genes available for genetic reassortment with the circulating human viruses (9). The lack of protective immunity in the human population against new HA and/or NA proteins can result in rapid global spread of the virus. In recent history, the emergence of high pathogenicity avian influenza viruses in domestic poultry and the increasing number of cases of direct transmission of avian influenza viruses to humans represent a major risk, confirmed by the ongoing outbreak of high pathogenicity avian influenza H5N1 viruses in the bird population, which has caused a nearly 50% case fatality rate among the people infected (10, 11). In addition, the highly contagious A H1N1 swine flu that recently emerged in Mexico has rapidly spread worldwide, representing a new threat to global human health. Novel antiviral drugs effective against different strains of influenza viruses are therefore greatly needed.

tein receptor; PBS, phosphate-buffered saline; PMSF, phenylmethylsulfonyl fluoride; PIC, protease inhibitor mixture; eIF, eukaryotic initiation factor; HAU, hemagglutinating units.

\* This work was supported by Romark Laboratories, LC and by the Italian Ministry of University and Scientific Research.

<sup>S</sup> The on-line version of this article (available at <http://www.jbc.org>) contains supplemental Figs. S1–S3.

<sup>1</sup> Present address: Research Center, San Pietro Hospital, Fatebenefratelli, 00189 Rome, Italy.

<sup>2</sup> To whom correspondence should be addressed: Dept. of Biology, University of Rome Tor Vergata, Via della Ricerca Scientifica, 00133 Rome, Italy. Tel.: 39-06-7259-4822; Fax: 39-06-7259-4821; E-mail: [santoro@bio.uniroma2.it](mailto:santoro@bio.uniroma2.it).

<sup>3</sup> The abbreviations used are: HA, hemagglutinin; NTZ, nitazoxanide; TIZ, tizoxanide; TM, tunicamycin; Endo-H, endo- $\beta$ -N-acetylglucosaminidase H; PNGase-F, peptide N-glycosidase F; MDCK, Madin-Darby canine kidney; p.i., post-infection; MTT, 3-(4,5-dimethylthiazol-2-yl)-2,5-diphenyltetrazolium bromide; GFP, green fluorescent protein; LDLR, low density lipopro-

Herein we document the anti-influenza activity of nitazoxanide (NTZ), a thiazolide anti-infective licensed in the United States (Alinia<sup>®</sup>; Romark Laboratories, Tampa, FL) for treating enteritis caused by *Cryptosporidium parvum* and *Giardia lamblia* in children and adults (12–14), its active circulating metabolite tizoxanide (2-hydroxy-*N*-(5-nitro-2-thiazolyl)benzamide) (TIZ) (see Fig. 1A), and second generation thiazolides.

## EXPERIMENTAL PROCEDURES

**Cell Culture, Treatment, and Transfection**—Madin-Darby canine kidney (MDCK), human A549 alveolar type II-like epithelial, Jurkat T-lymphoblastoid, and U397 monocytic leukemia cells were grown at 37 °C in a 5% CO<sub>2</sub> atmosphere in RPMI 1640 (Invitrogen), supplemented with 10% fetal calf serum, 2 mM glutamine, and antibiotics. NTZ, TIZ, second generation thiazolides (provided by Romark Laboratories), and swainsonine (Sigma-Aldrich) were dissolved in dimethyl sulfoxide; tunicamycin (TM) and 1-deoxymannojirimycin (Sigma-Aldrich) were dissolved in aqueous solution. Compounds were added immediately after a 1-h adsorption period and kept in the culture medium for the entire time of the experiment, unless differently specified. Controls received equal amounts of vehicle, which did not affect cell viability or virus replication. Cell viability was determined by the 3-(4,5-dimethylthiazol-2-yl)-2,5-diphenyltetrazolium bromide (MTT) to MTT formazan conversion assay (Sigma-Aldrich) as described previously (15). Microscopical examination of mock infected or virus-infected cells was performed using a Leica DM-IL microscope, and images were captured on a Leica DC 300 camera using Leica Image-Manager500 software.

For transfection experiments, MDCK cells plated in Lab-TekII coverglass chambers (Nunch-Thermo Fisher Scientific Inc.) were transiently transfected with green fluorescent protein (GFP)-tagged internalization-defective human low density lipoprotein receptor (LDLR) mutant (LDLR-A18-GFP plasmid, kindly provided by E. Rodriguez-Boulan, Cornell University, New York, NY), using Lipofectamine 2000 (Invitrogen) according to the manufacturer's instructions.

**Virus Preparation, Infection, and Titration**—Four different influenza A viruses, the mammalian H1N1 A/PR/8/34 (PR8) and A/WSN/33 (WSN), and H3N2 A/Firenze/7/03 (A/FI), and the H5N9 low pathogenicity avian strain A/Ck/It/9097/97 (A/Ck), as well as influenza B virus, B/Parma/3/04 clinical isolate, were utilized for this study. The A/Firenze/7/03, A/Ck/It/9097/97, and B/Parma/3/04 influenza viruses were a kind gift from Dr. Isabella Donatelli (Istituto Superiore di Sanità, Rome, Italy). The avian strain A/Ck/It/9097/97 was isolated after an initial passage of chicken organ homogenates into 10-day-old specific pathogen-free embryonated chicken eggs (16). Influenza A viruses were grown in the allantoic cavity of 8-day-old embryonated eggs. After 48 h at 37 °C, the allantoic fluid was harvested and centrifuged at 5000 rpm for 30 min to remove cellular debris, and virus titers were determined by hemagglutinin titration and plaque assay, according to standard procedures (8, 17). Confluent cell monolayers were infected with influenza virus for 1 h at 37 °C at a multiplicity of infection of 5 HAU/10<sup>5</sup> cells, unless differently specified. After the adsorption period (time 0), the viral inoculum was removed, and cell

monolayers were washed three times with phosphate-buffered saline (PBS). The cells were maintained at 37 °C in RPMI 1640 culture medium containing 2% fetal calf serum. For multistep virus growth curves, the infected cells were incubated in the same medium containing 1 μg/ml trypsin IX (Sigma-Aldrich). Virus yield was determined 24 or 48 h post-infection (p.i.) by hemagglutinin titration (8). For PR8 virus infectivity assay, MDCK cells grown on 96-well plates were inoculated with serial dilutions of viral suspension in the presence of 1 μg/ml trypsin for 48 h at 37 °C, and TCID<sub>50</sub> (50% tissue culture infective dose) was determined as described (17). Alternatively, virus titers were determined on MDCK cells by counting the numbers of fluorescent cells after infection and indirect immunofluorescence staining with anti-influenza A/PR/8/34 antibodies (anti-PR8, a kind gift from E. Rodriguez-Boulan, Cornell University). Titters were correspondingly expressed as fluorescence-forming units/ml.

For rhinovirus infection, confluent monolayers of cervical carcinoma HeLa cells (HeLa R19 cell line, kindly provided by Dr. A. Salvati, Istituto Superiore di Sanità) were infected with human rhinovirus type 2 for 1 h at 33 °C at 3 TCID<sub>50</sub>/cell. After the adsorption period, the viral inoculum was removed, and the cell monolayers were washed three times with medium without fetal calf serum and maintained at 33 °C in Dulbecco's modified Eagle's medium containing 2% fetal calf serum. Virus yield was determined at 24 h p.i. after three cycles of freezing-thawing by TCID<sub>50</sub> assay. Mock infected cells were treated identically and processed for cytotoxicity MTT assay at the same time.

**Metabolic Labeling, Analysis of Protein Synthesis, and Western Blot**—Mock infected or influenza virus-infected cells were labeled with 10 μCi/ml of [<sup>35</sup>S]Met/Cys (Redivue Pro-Mix <sup>35</sup>S *in vitro* cell labeling mix; GE Healthcare) for the indicated times after 30 min of starvation in methionine/cysteine-free medium. For pulse/chase experiments, the cells were labeled with [<sup>35</sup>S]Met/Cys (100 μCi/ml) for 15 min, after 30 min of starvation in methionine/cysteine-free medium. At the end of pulse, the cells were chased in complete medium containing 10 mM cold methionine and 1 mM cycloheximide for different times in the absence or presence of TIZ. The pulse/chase were terminated by placing the cells on ice. After cell lysis in RIPA (radioimmune precipitation assay) buffer (150 mM NaCl, 10 mM Tris-HCl, pH 7.5, 4 mM EDTA, 1% Triton X-100, 600 mM KCl), containing 1 mM phenylmethylsulfonyl fluoride (PMSF) and a protease inhibitor mixture (PIC; Roche Applied Science), samples containing the same amount of radioactivity were separated by SDS-PAGE (3% stacking gel, 10% resolving gel) and processed for autoradiography, as described (17). Autoradiographic patterns were visualized and quantified in a Typhoon-8600 Imager (Molecular Dynamics Phosphor-Imager<sup>TM</sup> (MDP)), and images were acquired using ImageQuant software (Amersham Biosciences) (MDP analysis).

For analysis of proteins incorporated into virus particles, PR8-infected or mock infected MDCK cells treated with TIZ, TM, or vehicle after virus adsorption were labeled at 3 h p.i. with [<sup>35</sup>S]Met/Cys (25 μCi/ml, 21-h pulse) in the presence of the drugs. At 24 h p.i., the cell culture supernatants were harvested, subjected to centrifugation at 13,000 rpm for 10 min to remove cellular debris, and then subjected to ultracentrifuga-

## Thiazolides Inhibit Influenza Virus HA Maturation

tion at 45,000 rpm (Beckman XL-100K Ultracentrifuge, rotor 70.1Ti; Beckman Coulter Inc.) for 2 h. The pellets containing viral particles were resuspended in Laemmli sample buffer, and radiolabeled viral proteins were separated by 10% SDS-PAGE and examined by autoradiography, after exposure to Amplify<sup>TM</sup> fluorographic reagent (GE Healthcare). Autoradiographic patterns were visualized as described above.

For Western blot analysis, the cells were lysed with cold high salt extraction buffer (18), containing 2 mM dithiothreitol, 1 mM PMSF, 1 mM orthovanadate, 20 mM  $\beta$ -glycerophosphate, 1 mM *p*-nitrophenyl phosphate, and PIC or with RIPA buffer containing 1 mM PMSF and PIC. Whole cell extracts (30  $\mu$ g) were separated by SDS-PAGE and blotted to nitrocellulose, and filters were incubated with polyclonal anti-Ser(P)<sup>51</sup>-eIF2 $\alpha$  (p-eIF2 $\alpha$ ; Calbiochem), anti-eIF2 $\alpha$  (FL-315; Santa Cruz Biotechnology), and anti-influenza A/PR/8/34 antibodies or monoclonal anti-HA (IVC102; Biodesign Inc.) and anti-Grp78/BiP (Stressgene) antibodies, followed by decoration with peroxidase-labeled anti-rabbit IgG or anti-mouse IgG (SuperSignal detection kit; Pierce). Quantitative evaluation of proteins was determined by Versadoc-1000 analysis using the Quantity One software program (Bio-Rad) (19).

**Immunoprecipitation of HA0**—PR8-infected or mock infected MDCK cells treated with 10  $\mu$ g/ml TIZ or control diluent after virus adsorption were labeled at 5 or 6 h p.i. with [<sup>35</sup>S]Met/Cys (70  $\mu$ Ci/ml, 4-h pulse) after 30 min of starvation in methionine/cysteine-free medium. After lysis in RIPA buffer in the presence of PIC and 1 mM PMSF, cell debris were removed by cold centrifugation at 13,000 rpm for 10 min. Radiolabeled lysates (50  $\mu$ l) were incubated with anti-HA monoclonal antibodies (IVC102; Biodesign Inc.) in RIPA buffer containing 1 mM PMSF, PIC, and protein A-Sepharose (Sigma-Aldrich) at 4 °C for 16 h. After centrifugation, the pellets were washed three times with RIPA buffer and eluted in Laemmli sample buffer (20) at 95 °C for 5 min. Immunoprecipitated samples were subjected to endoglycosidase H (Endo-H) digestion (as described below) and/or processed for SDS-PAGE (3% stacking gel, 10% resolving gel) and autoradiography, after exposure to Amplify<sup>TM</sup> fluorographic reagent. Autoradiographic patterns were visualized in Typhoon-8600 Imager, and the images were acquired as described above.

**Analysis of Hemagglutinin Glycosylation, Trimerization, and Processing**—Mock infected or influenza virus-infected cells were labeled with 20  $\mu$ Ci/ml of [<sup>3</sup>H]mannose or [<sup>3</sup>H]glucosamine hydrochloride (GE Healthcare) for 4 h at 6 h p.i. and then processed for SDS-PAGE (3% stacking gel, 10% resolving gel) and autoradiography, as described above. For endoglycosidase digestion experiments, MDCK cells were infected with PR8 influenza virus, washed free of unbound virus, and incubated in the presence or absence of 10  $\mu$ g/ml TIZ. At 5 h p.i. the cells were labeled with [<sup>35</sup>S]Met/Cys (50  $\mu$ Ci/ml, 4-h pulse) after 30 min of starvation in methionine/cysteine-free medium. At the end of pulse, the radioactive medium was removed, and cells were placed on ice. After lysis in L buffer (100 mM NaCl, 10 mM Tris-HCl, pH 7.5, 5 mM EDTA, 1% Triton X-100, 0.1% SDS) in the presence of PIC and 1 mM PMSF and cold centrifugation at 13,000 rpm for 10 min, samples containing the same amount of radioactivity were processed for Endo-H or peptide *N*-glycosi-

dase F (PNGase-F) digestion. For Endo-H digestion, the samples immunoprecipitated with anti-HA monoclonal antibodies (as described above) or nonimmunoprecipitated samples were incubated in 100  $\mu$ l of 0.1% SDS and 140 mM  $\beta$ -mercaptoethanol in 100 mM sodium citrate (pH 5.5) and heated for 5 min at 95 °C. After addition of 1 mM PMSF and PIC, the samples were divided into two equal aliquots, and one aliquot was incubated with 5 milliunits of Endo-H (Roche Applied Science) for 16 h at 37 °C. Peptide *N*-glycosidase digestion was performed with 500 units of PNGase-F, according to the manufacturer's protocol (New England BioLabs Inc.). Digestions were terminated with the addition of Laemmli sample buffer. The samples were heated at 95 °C for 5 min before loading onto 10% SDS-PAGE gels.

For analysis of trimer formations, cross-linking of HA was performed by adding 1:10 volume of dimethyl sulfoxide containing 0.2 mM ethylene glycol bis(succinimidylsuccinate) (Pierce) to whole cell extracts from mock infected and PR8-infected MDCK cells. After 15 min at 22 °C, the reactions were quenched by the addition of glycine at a final concentration of 75 mM, and the samples were subjected to SDS-PAGE (6% resolving gel) (21). The HA-cross-linked products were visualized by probing with monoclonal anti-HA antibodies or polyclonal anti-PR8.

**Immunofluorescence Microscopy**—PR8-infected MDCK and WSN-infected A549 cells grown on coverslips were fixed with 4% paraformaldehyde in phosphate-buffered saline for 20 min at room temperature at 16 or 24 h p.i., respectively. Mock infected cells were processed similarly. Fixed cells were either incubated with anti-HA monoclonal antibodies (IVC102; Biodesign Inc.) for 1 h at 37 °C for plasma membrane staining or were permeabilized with 0.1% Triton X-100-PBS for 10 min at room temperature and then incubated with monoclonal anti-HA and anti-p230 *trans*-Golgi (clone 15; BD Biosciences) or polyclonal anti- $\alpha$ -tubulin (11H10; Cell Signaling, Technology Inc.) antibodies for 1 h at 37 °C, followed by decoration with Alexa Fluor488-conjugated (Molecular Probes-Invitrogen) or rhodamine-conjugated (Pierce) goat anti-mouse IgG, and rhodamine-conjugated goat anti-rabbit IgG (Pierce). The nuclei were stained with 4',6-diamidino-2-phenylindole or Hoechst 33342 (Molecular Probes, Invitrogen). The images were captured and deconvolved with a DeltaVision microscope (Applied Precision) using the SoftWoRx-2.50 software (Applied Precision). Control incubations demonstrated non-cross-reactivity between the anti-immunoglobulin conjugates or between the anti-immunoglobulin conjugate and the irrelevant primary antibody. Images of a representative experiment of three with similar results are shown.

For detection of plasma membrane targeting of human LDLR, MDCK cells plated in coverglass chambers were transiently transfected with GFP-tagged internalization-defective human LDLR mutant (LDLR-A18-GFP plasmid) and, after 8 h, treated with TIZ (10  $\mu$ g/ml) or vehicle for the following 16 h. After blocking protein synthesis with 100  $\mu$ g/ml cycloheximide (Sigma-Aldrich) for 1 h, the plasma membranes were stained using CellMask<sup>TM</sup> Orange plasma membrane stain (Molecular Probes, Invitrogen). After staining, the cells were examined using a Leica DM-IL fluorescence microscope equipped with

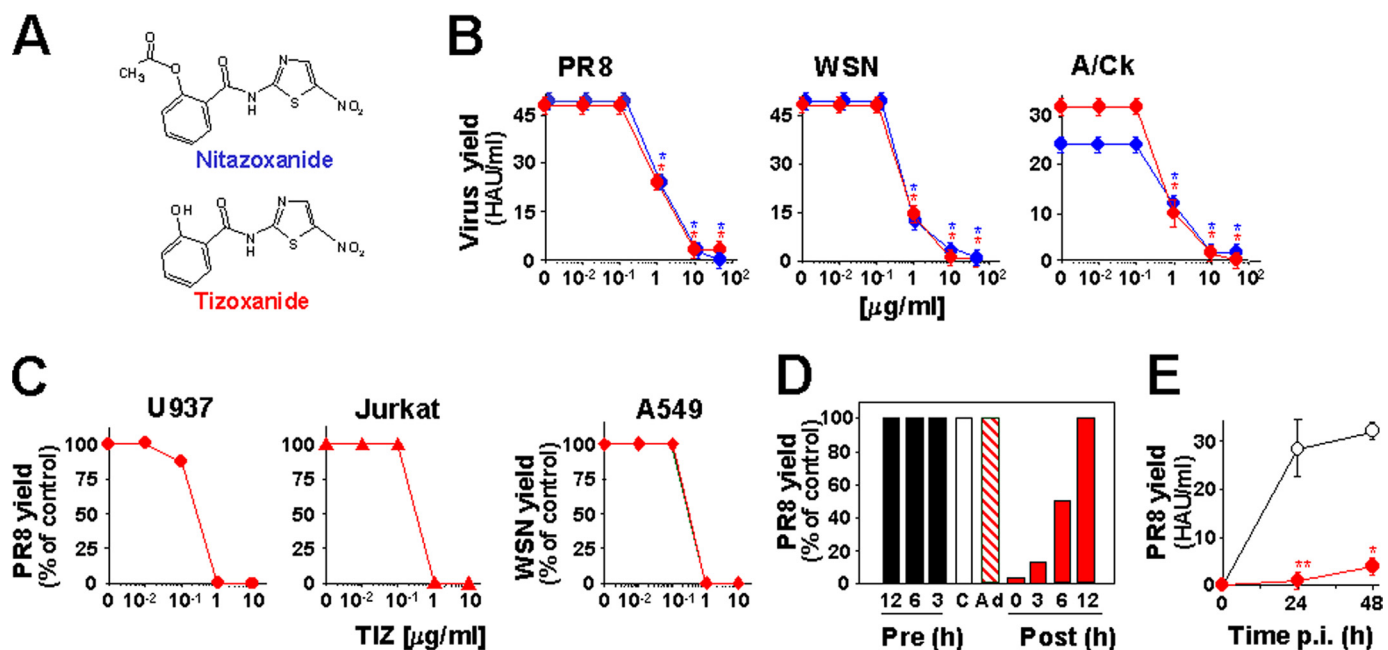


FIGURE 1. **Thiazolides inhibit influenza A virus replication acting at a post-entry level.** *A*, structure of NTZ and TIZ. *B*, NTZ (blue circles) and TIZ (red circles) inhibit the replication of mammalian (PR8 and WSN) and avian (A/Ck) influenza A virus strains in MDCK cells. Virus yield was determined at 24 h p.i. *C*, antiviral activity of TIZ on influenza A PR8 virus in human monocytic U937 (●) and T-lymphoblastoid Jurkat (▲) cells and WSN virus in human lung epithelial A549 cells (◆). *D*, MDCK cells were treated with 10  $\mu\text{g/ml}$  TIZ (filled bars) at the indicated times before infection (Pre), immediately after the adsorption period (Post), or only during the adsorption period (Ad, dashed bar). The empty bar represents untreated infected control (C). *E*, long term antiviral activity of TIZ in PR8-infected MDCK cells treated with 10  $\mu\text{g/ml}$  TIZ (filled circles) or vehicle (empty circles) after virus adsorption. *B–E*, virus yield, expressed in HAU/ml (*B* and *E*) or as a percentage of untreated control (*C* and *D*), represents the means  $\pm$  S.D. of duplicate samples from a representative experiment of three with similar results. \*,  $p < 0.01$ ; \*\*,  $p < 0.05$ .

UV excitation filters. The images were captured with a Leica DC-300 camera using Leica Image-Manager500 software.

**Hemadsorption Assay**—Mock or PR8-infected MDCK cell monolayers were treated with TIZ, TM, or vehicle after virus adsorption. At 5 h p.i., the cells were washed three times with PBS and incubated with 0.1% of human red blood cells in PBS for 20 min at 4 °C to inhibit neuraminidase activity. After removal of unbound erythrocytes by washing three times with PBS, red blood cells adsorbed on MDCK cell surface were detected by phase contrast microscopy. The images were captured with a Leica DMLB microscope equipped with a Leica DC300 camera, using Leica Image-Manager500 software. Adherent erythrocytes were lysed in 150 mM  $\text{NH}_4\text{Cl}$  buffer for 2 h at room temperature and quantified by measuring hemoglobin absorbance at  $\lambda = 540$  nm (22).

**Statistical Analysis**—Statistical analysis was performed using Student's *t* test for unpaired data. The data are expressed as the means  $\pm$  S.D. of duplicate samples. *p* values of  $<0.05$  were considered significant.

## RESULTS

**Antiviral Activity of Thiazolides against Different Strains of Influenza A Virus**—The effect of thiazolide treatment was investigated in human and canine cells after infection with four different strains of influenza A virus: the mammalian H1N1 A/PR/8/34 (PR8) and A/WSN/33 (WSN), and H3N2 A/Firenze/7/03 (A/FI) viruses, and the H5N9 low pathogenicity avian strain A/Ck/It/9097/97 (A/Ck). MDCK cells infected with PR8, WSN, or A/Ck influenza viruses were treated with different concentrations of NTZ, TIZ, or vehicle

immediately after the virus adsorption period, and virus yield was determined at 24 h p.i. NTZ treatment caused a dose-dependent inhibition of virus replication with  $\text{EC}_{50}$  (effective concentration 50%) values of 1, 0.5, and 1  $\mu\text{g/ml}$  for PR8, WSN, and A/Ck viruses, respectively (Fig. 1*B*). TIZ was equally active against all influenza A strains with an  $\text{EC}_{50}$  of 1  $\mu\text{g/ml}$  (PR8) and 0.5  $\mu\text{g/ml}$  (WSN and A/Ck) (Fig. 1*B*). TIZ was also very effective in inhibiting the replication of H3N2 A/FI influenza A and B/Parma/3/04 influenza B viruses (supplemental Fig. S1, *A* and *B*). Neither NTZ nor TIZ were cytotoxic at the effective antiviral concentration for uninfected cells ( $\text{CC}_{50}$  (cytotoxic concentration 50%)  $> 50$   $\mu\text{g/ml}$ ). In addition to the canine MDCK cells typically used for influenza virus studies, TIZ was effective in inhibiting influenza A virus replication at submicromolar ( $\text{EC}_{50} = 0.3$   $\mu\text{g/ml}$ ) nontoxic concentrations in different types of human cells, including monocytic U937, T-lymphocytic Jurkat, and alveolar type II-like A549 cells (Fig. 1*C*). The anti-influenza activity of TIZ was independent of the multiplicity of infection, and a dramatic block of H1N1 PR8 virus replication was equally detected under conditions of multi- and single-step virus growth (supplemental Fig. S1, *C* and *D*). In addition to NTZ and TIZ, the antiviral activity of different second generation thiazolides against PR8 influenza A virus is described in Table 1. Among the novel thiazolides tested, the compound RM5014 was found to be 10 times more effective than NTZ and TIZ, with  $\text{EC}_{50} = 0.1$   $\mu\text{g/ml}$  and  $\text{CC}_{50} > 50$   $\mu\text{g/ml}$ .

**Thiazolides Act at a Post-entry Level**—To investigate whether thiazolide treatment before virus adsorption could protect host cells from viral infection, MDCK cells were

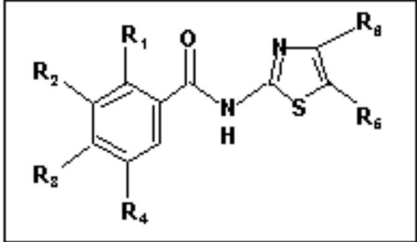
## Thiazolides Inhibit Influenza Virus HA Maturation

**TABLE 1**

**Anti-influenza activity of thiazolides**

A, schematic structure of thiazolides. B, evaluation of the anti-influenza activity of the novel thiazolides RM4803, RM4832, RM4850, RM4865, and RM5014 as compared to NTZ and TIZ. Mock-infected or PR8-infected MDCK cells were treated with different concentrations (0.01, 0.1, 1, 10, and 50  $\mu\text{g/ml}$ ) of the compounds immediately after the virus adsorption period. Cell viability and virus yield were determined at 24 h p.i. by MTT assay and hemagglutination assay, respectively. The data, expressed as  $\text{EC}_{50}$  and  $\text{CC}_{50}$ , represent the means  $\pm$  SD of triplicate experiments. The lack of SD in the  $\text{CC}_{50}$  column indicates that the values were identical.

**A**



**B**

	$\text{EC}_{50}$ [ $\mu\text{g/ml}$ ]	$\text{CC}_{50}$ [ $\mu\text{g/ml}$ ]
<b>Nitazoxanide</b> R <sub>1</sub> =OCOCH <sub>3</sub> R <sub>2</sub> =H R <sub>3</sub> =H R <sub>4</sub> =H R <sub>5</sub> =NO <sub>2</sub> R <sub>6</sub> =H	1.00 $\pm$ 0.01	>50
<b>Tizoxanide</b> R <sub>1</sub> =OH R <sub>2</sub> =H R <sub>3</sub> =H R <sub>4</sub> =H R <sub>5</sub> =NO <sub>2</sub> R <sub>6</sub> =H	1.00 $\pm$ 0.01	>50
<b>RM4803</b> R <sub>1</sub> =OCOCH <sub>3</sub> R <sub>2</sub> =CH <sub>3</sub> R <sub>3</sub> =H R <sub>4</sub> =H R <sub>5</sub> =Br R <sub>6</sub> =H	1.00 $\pm$ 0.01	>50
<b>RM4832</b> R <sub>1</sub> =OH R <sub>2</sub> =H R <sub>3</sub> =H R <sub>4</sub> =H R <sub>5</sub> =Br R <sub>6</sub> =H	1.25 $\pm$ 0.35	>50
<b>RM4850</b> R <sub>1</sub> =OH R <sub>2</sub> =H R <sub>3</sub> =H R <sub>4</sub> =CH <sub>3</sub> R <sub>5</sub> =Cl R <sub>6</sub> =H	4.00 $\pm$ 0.01	>50
<b>RM4865</b> R <sub>1</sub> =OCOCH <sub>3</sub> R <sub>2</sub> =H R <sub>3</sub> =H R <sub>4</sub> =CH <sub>3</sub> R <sub>5</sub> =Cl R <sub>6</sub> =H	2.00 $\pm$ 1.41	>50
<b>RM5014</b> R <sub>1</sub> =OCOCH <sub>3</sub> R <sub>2</sub> =H R <sub>3</sub> =H R <sub>4</sub> =H R <sub>5</sub> =H R <sub>6</sub> =SO <sub>2</sub> CH <sub>3</sub>	0.10 $\pm$ 0.01	>50

treated with 10  $\mu\text{g/ml}$  TIZ for 12, 6, or 3 h. At the indicated times the drug was removed, and cell monolayers were washed three times before infection with PR8 virus. As shown in Fig. 1D (*Pre*), tizoxanide pretreatment of cells up to 12 h before viral infection had no effect on influenza virus replication. Moreover, treatment of the viral inoculum (data not shown) or treatment of cells only during the adsorption period did not inhibit virus replication (Fig. 1D), indicating that the drug is not directly affecting virus infectivity, nor its binding or entry into target cells. TIZ treatment initiated between 0 and 3 h p.i. was the most effective in inhibiting virus replication (Fig. 1D, *Post*). Treatment started at 6 h p.i. was less effective but still able to inhibit virus replication, whereas the drug was ineffective when administered at 12 h p.i. A single administration of the drug after virus adsorption was effective in inhibiting virus replication for at least 48 h after infection (Fig. 1E).

**Thiazolides Selectively Alter Viral Hemagglutinin Maturation**—To investigate whether the anti-influenza activity of thiazolides was caused by protein synthesis alterations, mock infected or PR8-infected cells treated with TIZ soon after virus adsorption were labeled with [<sup>35</sup>S]Met/Cys at different times p.i., and the proteins were analyzed by SDS-PAGE and autoradiography or Western blot analysis. As shown in Fig. 2A, TIZ did not inhibit host protein synthesis (*bottom panels*) nor cause detectable alterations in the electrophoretic pattern of the synthesized polypeptides (*top panels*); in addition, TIZ did not affect phosphorylation of eIF2- $\alpha$  (*middle panels*) in either uninfected or PR8-infected cells. The main influenza virus proteins were found to be synthesized in large amounts in untreated cells starting at 4 h p.i.; no major changes in influenza virus protein synthesis were detected in treated cells, with the exception of the disappearance of a band of  $\sim$ 79-kDa molecular mass, subsequently identified as the mature isoform of the hemagglutinin precursor, and the simultaneous appearance of a faster migrating band of 74 kDa (Fig. 2A).

To determine whether TIZ treatment selectively alters HA synthesis, mock infected or PR8-infected MDCK cells treated with TIZ (10  $\mu\text{g/ml}$ ) were metabolically labeled at 5 h p.i. (4-h pulse), and radiolabeled proteins were immunoprecipitated with anti-hemagglutinin monoclonal antibodies and then processed for SDS-PAGE and autoradiography. Data shown in Fig. 2B identify the protein whose electrophoretic mobility is altered by TIZ as the viral HA0 precursor. To determine whether the TIZ-induced HA0 modification was transient, mock infected or PR8-infected MDCK cells treated with TIZ (10  $\mu\text{g/ml}$ ) or the *N*-glycosylation inhibitor TM (5  $\mu\text{g/ml}$ ) were metabolically labeled at 3 h p.i. for the next 15 h, and proteins were analyzed by SDS-PAGE and autoradiography. Alternatively, PR8-infected cells were labeled at 5 h p.i. and then chased in the presence of 10 mM cold methionine and 1 mM cycloheximide for the next 3 h p.i. As shown in Fig. 2C, TIZ-induced HA0 post-translational modification was still evident at 18 h p.i. and appeared to differ from TM-induced alteration, as indicated by a different electrophoretic mobility pattern of the two HA0 forms; in addition, whereas TM caused a decrease in HA0 accumulation, as previously described (23), prolonged TIZ treatment did not reduce intracellular HA0 levels in infected cells. Differently from TM, TIZ did not induce the expression

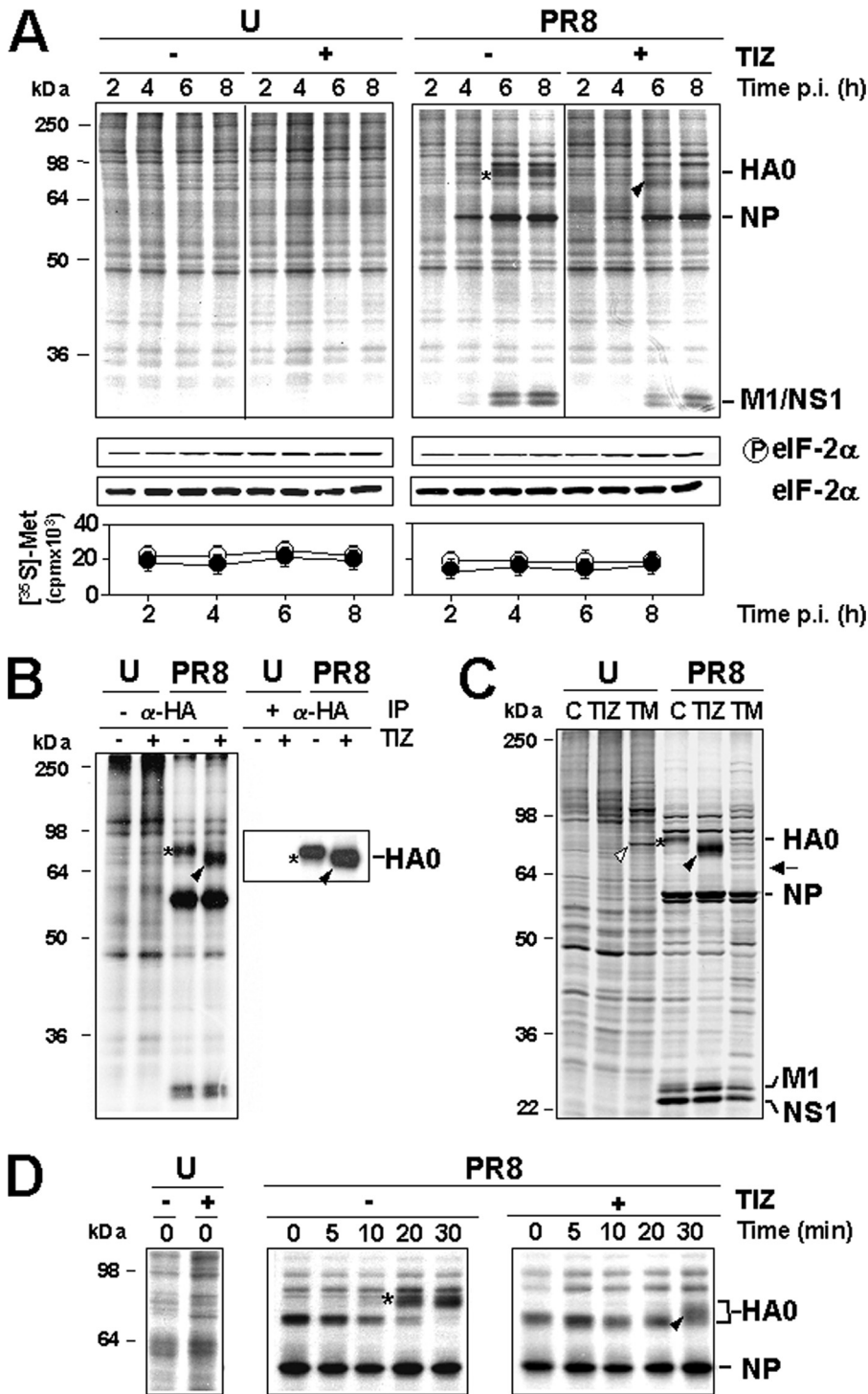


**FIGURE 2. Tizoxanide selectively alters influenza hemagglutinin maturation.** *A*, effect of TIZ on the kinetics of PR8 virus protein synthesis. Autoradiography of [<sup>35</sup>S]Met/Cys-labeled proteins (1.5-h pulse) at different times p.i. from mock infected (U) or PR8-infected cells treated with 10 μg/ml TIZ after virus adsorption (*top panels*). The viral proteins are indicated. In the same experiment, protein synthesis was determined by [<sup>35</sup>S]Met/Cys incorporation into proteins of cells treated with TIZ (●) or vehicle (○) (*bottom panels*), and phospho-eIF2α protein levels were determined by immunoblot analysis using anti-Ser(P)<sup>51</sup>-eIF2α (p-eIF2α) or eIF2α panspecific antibodies (*middle panels*). *B*, hemagglutinin identification by immunoprecipitation with anti-HA antibodies after [<sup>35</sup>S]Met/Cys labeling at 5 h p.i. (4-h pulse). Immunoprecipitated proteins (+α-HA, IP) and radiolabeled proteins from the same samples before antibody addition (−α-HA) are shown. Positions of HA uncleaved precursor (HA0) are indicated. *C*, autoradiography of [<sup>35</sup>S]Met/Cys-labeled proteins (1.5-h pulse) from mock infected (U) or PR8-infected cells treated with 10 μg/ml TIZ, 5 μg/ml TM, or vehicle (*lane C*) after virus adsorption. The white arrowhead and black arrow indicate TM-induced GRP78/BiP and nonglycosylated HA0 (identified by immunoblot; not shown), respectively. *D*, autoradiography of [<sup>35</sup>S]Met/Cys-labeled proteins (15-min pulse at 5 h p.i., followed by chase for the indicated times) from PR8-infected cells treated as in *A*. *A–D*, the slower- and faster-migrating HA0 forms in untreated or TIZ-treated cells are identified by asterisks and black arrowheads, respectively.

of the glucose-regulated stress protein Grp78/BiP, a marker of the unfolded protein response, in MDCK cells (Fig. 2C). Results from the chase experiment indicated that in untreated cells HA0 reached the mature 79-kDa form between 10 and 20 min after synthesis, whereas in the presence of TIZ the more slower migrating 74-kDa HA0 form started to appear later (30 min) after synthesis (Fig. 2D), and no further change in electrophoretic mobility was detectable in the next 2.5 h (data not shown).

To determine whether TIZ is inhibiting HA0 glycosylation, PR8-infected cells were treated with TIZ or tunicamycin after virus adsorption and, at 6 h p.i., were labeled with either [<sup>35</sup>S]Met/Cys, [<sup>3</sup>H]glucosamine, or [<sup>3</sup>H]mannose. As shown in Fig. 3A, whereas TM completely prevented HA0 glycosylation, treatment with TIZ did not decrease glucosamine and actually increased mannose incorporation into the immature HA0 form. However, the thiazolidine appears to act differently from the inhibitors of α-mannosidase I, 1-deoxymannojirimycin, and α-mannosidase II, swainsonine, as indicated by the different electrophoretic mobility of TIZ-induced immature HA0 as compared with the HA0 forms present in cells treated with the two inhibitors (Fig. 3B).

It is known that HA maturation is influenced both by the host cell glycosylation machinery (24) and the virus strain (25). To establish whether the described HA0 alteration was specific for PR8 virus or was cell-dependent, human lung epithelial A549 cells were infected with the influenza A human WSN strain, whereas MDCK cells were infected with the avian A/Ck strain. In both cases, alterations in HA0 maturation analogous to the ones described for the PR8 strain were detected (Fig. 3, C and D), indicating that TIZ is able to inhibit HA0 maturation, independently of the type of host cell and influenza A strain. Finally, as shown in Fig. 3 (E and F), nitazoxanide caused similar alter-

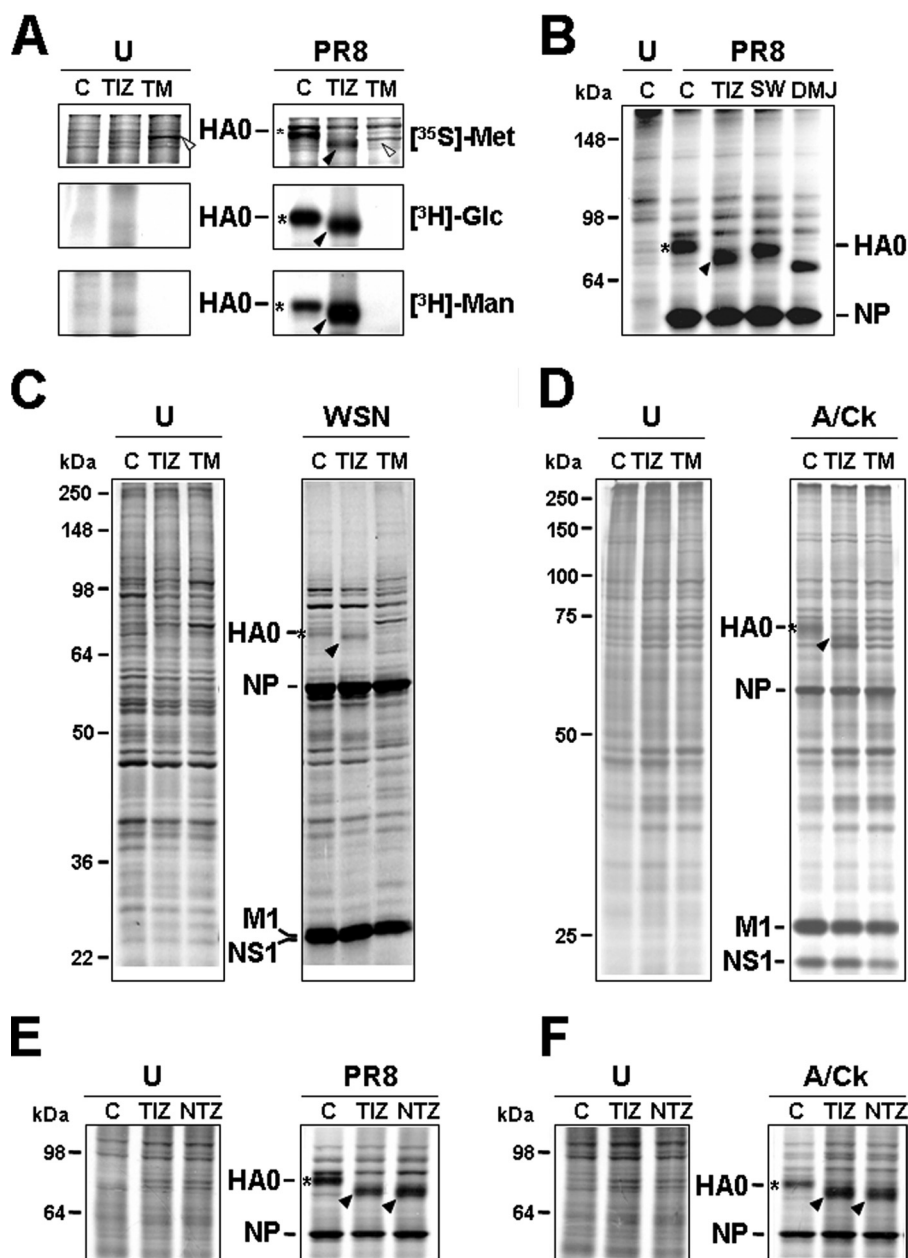


**FIGURE 3. Thiazolides interfere with viral hemagglutinin N-glycosylation.** *A*, mock infected (*U*) or PR8-infected MDCK cells were treated with 10 μg/ml TIZ, 5 μg/ml TM, or vehicle (*lane C*) after virus adsorption. At 6 h p.i., the cells were labeled for 4 h with [<sup>35</sup>S]Met/Cys (*top panels*), [<sup>3</sup>H]glucosamine (*middle panels*), or [<sup>3</sup>H]mannose (*bottom panels*). Radiolabeled samples were processed for SDS-PAGE and autoradiography. Sections of fluorograms from SDS-PAGE gels are shown. White arrowheads indicate TM-induced Grp78/BiP. *B*, mock infected (*U*) or PR8-infected MDCK cells were treated with 10 μg/ml TIZ, 10 μg/ml swainsonine (*SW*), 15 μg/ml 1-deoxymannojirimycin (*DMJ*), or vehicle (*lane C*) after virus adsorption. At 6 h p.i., the cells were labeled with [<sup>35</sup>S]Met/Cys (4-h pulse), and radiolabeled samples were processed for SDS-PAGE and autoradiography. *C* and *D*, autoradiography of radiolabeled proteins from mock infected (*U*) or WSN-infected A549 cells (*lane C*) and mock infected or avian influenza A virus-infected (A/Ck) MDCK cells (*D*) treated with 5 μg/ml TIZ, 5 μg/ml TM, or vehicle (*lane C*) after virus adsorption. At 3 h (WSN) or 6 h (A/Ck) p.i., the cells were labeled with [<sup>35</sup>S]Met/Cys for 15 h (WSN) or 4 h (A/Ck). *E* and *F*, autoradiography of radiolabeled proteins from mock infected (*U*), PR8-infected (*E*), or avian influenza A virus-infected (A/Ck) (*F*) MDCK cells treated with 10 μg/ml TIZ, 10 μg/ml NTZ or vehicle (*lane C*) after virus adsorption. At 6 h p.i., the cells were labeled with [<sup>35</sup>S]Met/Cys for 4 h. *A–F*, viral proteins HA0, NP, M1, and NS1 are indicated. The slower- and faster-migrating HA0 forms in untreated or thiazolide-treated cells are identified by asterisks and black arrowheads, respectively.

ations in the hemagglutinin of human (*E*) and avian (*F*) influenza viruses.

*Tioxanide Inhibits HA Transport to the Cell Membrane and Prevents Virus Exit from Host Cells*—Glycosylation of HA, like other cell surface glycoproteins, is initiated in the endoplasmic

reticulum, adding the “high mannose” oligosaccharides (26). The mannose-rich sugar component is processed in the Golgi apparatus during the transport to the cell surface, and terminal glycosylation occurs in *trans* cisternae of the Golgi apparatus (27). To investigate whether TIZ could affect HA0 passage through the Golgi, we subjected aliquots of radiolabeled proteins and HA0 immunoprecipitated samples to digestion with Endo-H, an enzyme that removes *N*-linked carbohydrate chains that have not been terminally glycosylated (28) or with PNGase-F, an enzyme that removes all *N*-glycans (29). As expected, both forms of the protein were sensitive to PNGase-F digestion; however, whereas HA0 from control cells was terminally glycosylated becoming Endo-H-resistant, HA0 from TIZ-treated cells remained sensitive to digestion with the protease up to 4 h after synthesis (Fig. 4, *A* and *B*). As shown in Fig. 4*C*, the TIZ-induced alterations did not prevent the ability of HA0 to form trimers.

Because acquisition of Endo-H resistance is a marker for transport into the *cis* and *middle* Golgi compartments (29), these results indicate that the TIZ-induced alteration may block HA0 trafficking between the endoplasmic reticulum and the Golgi complex, preventing its transport to the plasma membrane. Inhibition of transport to the *trans*-Golgi compartment was in fact detected by immunofluorescence using specific *trans*-Golgi antibodies (Fig. 4*D*). To confirm that TIZ treatment inhibited HA transport to the host cell plasma membrane, preventing the exit of mature viral particles, mock infected and PR8-infected MDCK cells were treated with TIZ (10 μg/ml) or tunicamycin (5 μg/ml) after virus adsorption, and levels of cytoplasmic (Fig. 5*A*) and plasma membrane (Fig. 5*B*) viral hemagglutinin were detected by immunofluorescence at 16 h p.i. These studies confirmed that, whereas HA0 cytoplasmic levels in TIZ-treated cells were similar to control (Fig. 5*A*), plasma membrane levels of the viral protein were dramatically decreased in TIZ-treated cells (Fig. 5*B*, *top row*). A substantial

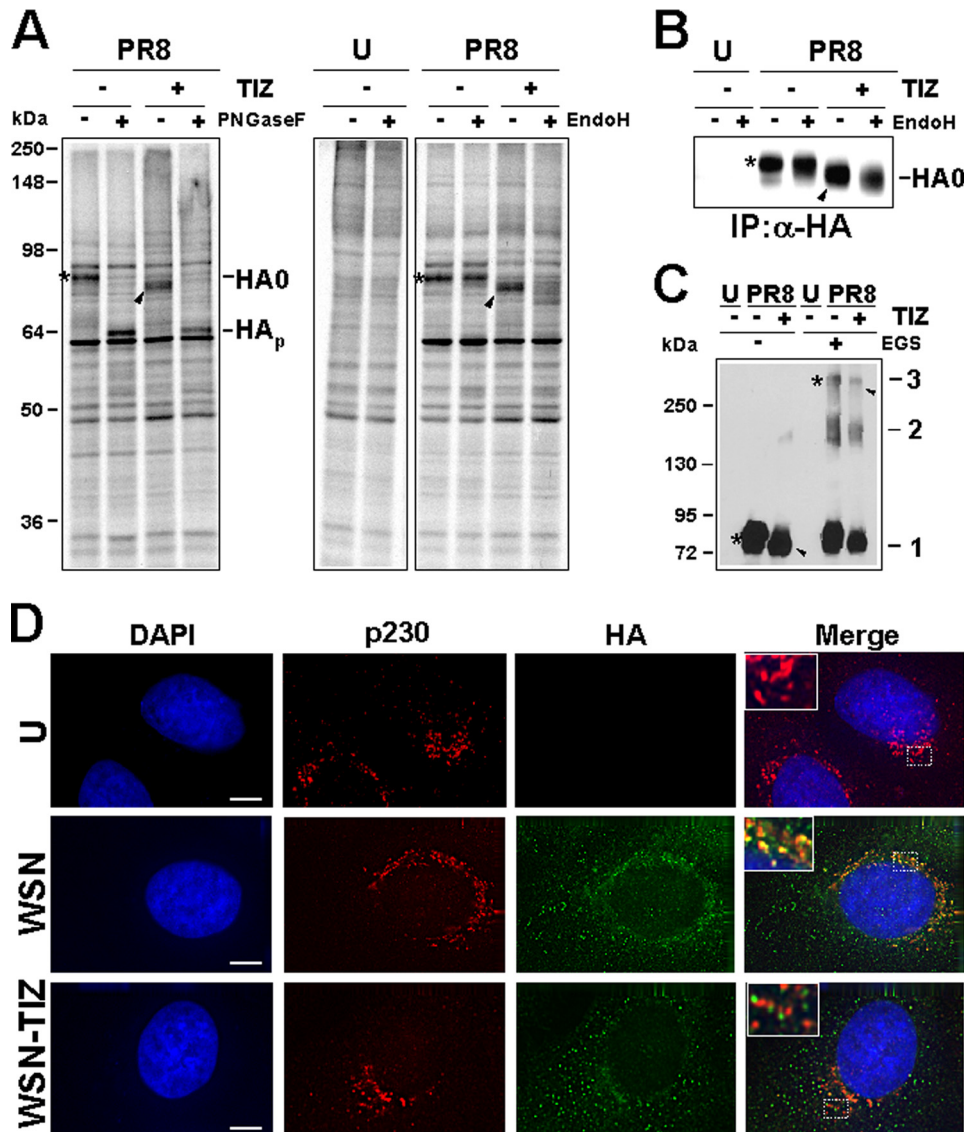
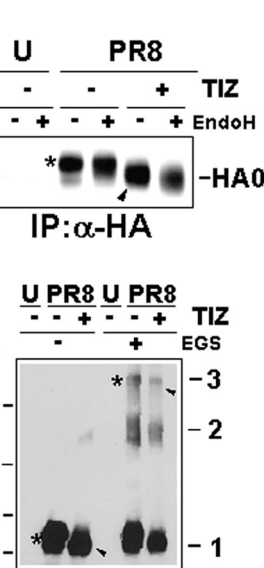


**FIGURE 4. Tizoxanide blocks HA maturation at an Endo-H-sensitive stage.** *A*, mock infected (*U*) or PR8-infected MDCK cells treated with 10  $\mu\text{g/ml}$  TIZ (+) or vehicle (–) after virus adsorption were labeled with [ $^{35}\text{S}$ ]Met/Cys (4-h pulse) at 5 h p.i. Radiolabeled proteins were digested (+) or not (–) with PNGase-F or Endo-H and processed for SDS-PAGE and autoradiography. Uncleaved glycosylated (*HA*<sub>0</sub>) and nonglycosylated (*HA*<sub>p</sub>) hemagglutinin precursor forms are indicated. *B*, MDCK cells treated as in *A* were labeled with [ $^{35}\text{S}$ ]Met/Cys (4-h pulse) at 6 h p.i. Radiolabeled proteins were immunoprecipitated (*IP*) with anti-HA antibodies ( $\alpha$ -HA), digested (+) or not (–) with Endo-H, and processed for SDS-PAGE. Sections of fluorograms are shown. *C*, whole cell extracts from mock infected (*U*) and PR8-infected MDCK cells treated with TIZ (+) or vehicle (–) were incubated with (+) or without (–) the cross-linking reagent ethylene glycol bis(succinimidylsuccinate) (*EGS*, 0.2 mM) and processed for Western blot using anti-HA antibodies. HA monomers (*mark 1*), dimers (*mark 2*), and trimers (*mark 3*) are indicated. *A–C*, slower- and faster-migrating *HA*<sub>0</sub> forms in untreated or TIZ-treated cells are identified by asterisks and black arrowheads, respectively. *D*, immunofluorescence of mock infected (*U*) and WSN-infected A549 cells treated with TIZ (5  $\mu\text{g/ml}$ ) or vehicle for 24 h, labeled with anti-p230 *trans*-Golgi (*red*) and anti-HA (*green*) antibodies. The nuclei are stained with 4',6-diamidino-2-phenylindole (*DAPI*, *blue*). The overlay of the three fluorochromes is shown (*merge*). The enlarged areas (*insets*) highlight the localization of HA in untreated and TIZ-treated cells. The images were captured and deconvolved with a DeltaVision microscope using SoftWoRx-2.50 software. Bar, 5  $\mu\text{m}$ .

decrease in HA plasma membrane levels after TIZ treatment was further confirmed by determining the biological function of plasma membrane-incorporated HA by receptor-binding (hemadsorption of erythrocytes) assay (Fig. 5*B*, bottom row). In parallel studies, after transient transfection of MDCK cells with a GFP-tagged internalization-defective human low density lipoprotein receptor mutant (LDLR-A18-GFP plasmid), it was found that TIZ did not inhibit plasma membrane targeting of



LDLR, suggesting a selective effect of thiazolides (supplemental Fig. S2). Similar results were obtained after transient transfection of MDCK cells and HEK-293 cells with a different plasma membrane cellular glycoprotein, the human Toll-like receptor-4 (data not shown).

In parallel samples, mock infected and PR8-infected cells were metabolically labeled with [ $^{35}\text{S}$ ]Met/Cys at 3 h p.i. for the next 21 h, and radiolabeled virions were purified from the supernatant of infected cells. Proteins incorporated into viral particles were analyzed by SDS-PAGE and autoradiography. As shown in Fig. 5*C*, viral proteins could not be detected in the supernatant of TIZ-treated cells. The dramatic reduction of viral particles was confirmed by determining virus yields from parallel, nonlabeled samples by TCID<sub>50</sub> infectivity assay (Fig. 5*D*, top panel) or HAU assay (Fig. 5*D*, bottom panel) at 24 h p.i. Finally, nitazoxanide and TIZ did not significantly affect the replication of the human rhinovirus type 2, a picornavirus whose maturation does not require viral protein trafficking to the cell membrane (supplemental Fig. S3).

## DISCUSSION

The emergence of highly pathogenic influenza A virus strains represents a serious threat to global human health. Efforts to control emerging influenza strains are focused on surveillance and early diagnosis, as well as on the development of effective vaccines and novel antiviral drugs. The obstacles in developing successful vaccines against emerging influenza viruses with pandemic potential have been recently reviewed (30). As for antiviral therapy, two classes of drugs are currently available for chemoprophylaxis and treatment of influenza. These include the NA inhibitors oseltamivir and zanamivir, which impair the efficient release of viruses from the infected host cell, and amantadine and rimantadine, which target the viral M2 protein required for virus uncoating (30, 31). Antiviral chemotherapy with M2 inhibitors reduces the duration of symptoms of clinical influenza, but major side effects were described (31). Novel sialic acid analogs have prophylactic effect; however, they only have



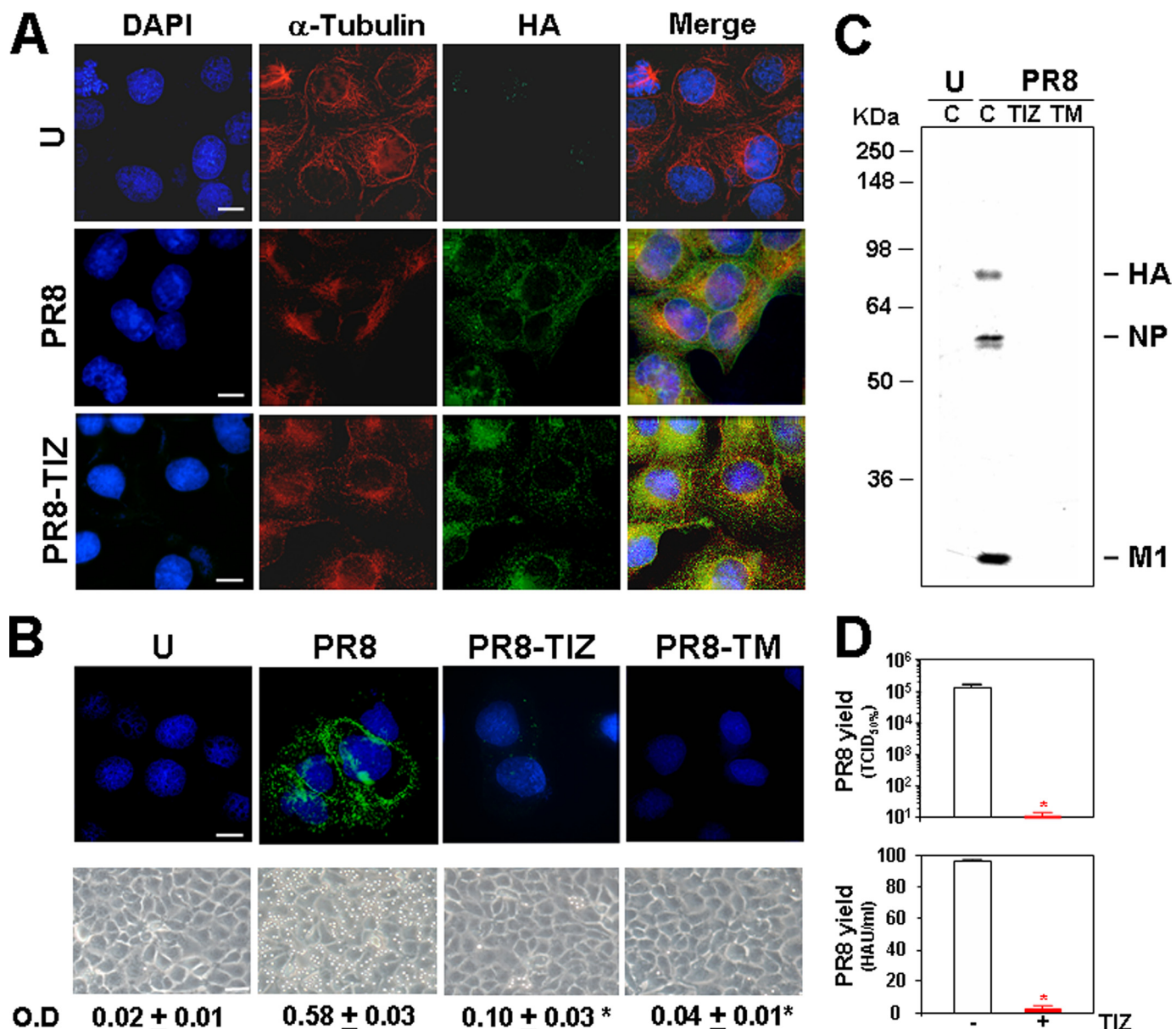


**FIGURE 5. Tizoxanide inhibits transport of influenza hemagglutinin to the cell surface.** *A*, levels of total hemagglutinin (green) and  $\alpha$ -tubulin (red) were detected in mock infected (U) and untreated or TIZ-treated (10  $\mu$ g/ml) PR8-infected MDCK cells at 16 h p.i. by indirect immunofluorescence (bar, 10  $\mu$ m). The nuclei are stained with 4',6-diamidino-2-phenylindole (DAPI, blue). The overlay of the three fluorochromes is shown (merge). The images were captured and deconvolved with a DeltaVision microscope using the SoftWoRx-2.50 software. *B*, levels of plasma-membrane hemagglutinin (green) were detected at 16 h p.i. by indirect immunofluorescence (top) in mock infected or PR8-infected cells treated with 10  $\mu$ g/ml TIZ or 5  $\mu$ g/ml TM. The nuclei are stained with Hoechst 33342 (blue). The images were processed as in *A* (bar, 10  $\mu$ m). The overlay of the two fluorochromes is shown. Erythrocytes hemadsorption on plasma membrane at 5 h p.i. is shown in parallel samples (bottom row) (bar, 35  $\mu$ m). Hemoglobin levels of bound erythrocytes were quantified spectrophotometrically ( $\lambda = 540$  nm). The data, expressed in optical density (O.D.), represent the means  $\pm$  S.D. of duplicate samples from a representative experiment of two with similar results. \*,  $p < 0.05$  versus infected-control. *C*, autoradiography of [<sup>35</sup>S]Met/Cys-labeled proteins incorporated into viral particles purified at 24 h p.i. from supernatants of mock infected or PR8-infected cells treated as in *B*. Viral proteins (HA, NP, and M1) are indicated. *D*, in parallel, virus yield was determined in untreated (empty bars) or TIZ-treated (filled bars) PR8-infected cells at 24 h p.i. by infectivity assay (top) and hemagglutination assay (bottom). The data, expressed in TCID<sub>50</sub>/ml and HAU/ml respectively, represent the means  $\pm$  S.D. of duplicate samples from a representative experiment of two with similar results. \*,  $p < 0.05$  versus infected control.

moderate therapeutic effects on shortening the infection (31). An additional obstacle to effective treatment of influenza with these drugs is represented by the high level drug resistance to both types of inhibitors, conferred by single amino acid substitutions in the M2 and NA proteins (31). For these reasons the disease is by no means under control, and novel antiviral drugs designed against different influenza virus targets are greatly needed, especially in view of the emergence of new virulent strains.

Herein we document that the anti-infective drug nitazoxanide and its active circulating metabolite tizoxanide possess potent anti-influenza A activity that is independent of the viral strain and/or the host-cell type. We also describe a group of novel thiazolides with anti-influenza activity. Among these, the compound RM5014 was found to be the most potent, being 10 times more active than the parent compound.

Importantly, these molecules act via a novel mechanism. The thiazolides do not affect virus infectivity, binding, or entry into

target cells and do not cause a general inhibition of viral protein expression, whereas they selectively block the maturation and intracellular transport of the viral hemagglutinin.

Influenza A virus hemagglutinin is a trimeric glycoprotein that contains three to nine *N*-linked glycosylation sequons/subunit, depending on the strain (32, 33). HA is initially synthesized and core-glycosylated in the endoplasmic reticulum as a 75–79-kDa precursor (HA0) that assembles into noncovalently linked homotrimers. The trimers are rapidly transported to the Golgi complex and reach the plasma membrane, where HA insertion initiates the process of assembly and maturation of the newly formed viral particles (33–35). Just prior to or coincident with insertion into the plasma membrane, each trimer subunit is proteolytically cleaved into two glycoproteins, HA1 and HA2, which remain linked by a disulfide bond (3).

By using different biochemical approaches, we show that TIZ blocks HA terminal glycosylation at a stage preceding resistance to endoglycosidase H digestion, which is a marker for transport into the *cis* and middle Golgi compartments (29). Immunomicroscopy studies and analysis of viral particles produced by infected cells confirm that the TIZ-induced alterations impair HA0 trafficking between the endoplasmic reticulum and the Golgi complex, preventing its transport and insertion into the host cell plasma membrane and blocking the exit of mature virions from host cells. Whether the alteration of HA maturation is caused by direct binding of TIZ to the viral glycoprotein or is due to a cell-mediated effect remains to be established.

Thiazolides have been shown to possess antiviral activity against two different RNA viruses: hepatitis C, a positive strand RNA virus, and rotavirus, a double-stranded RNA virus, and a DNA virus, the hepatitis B virus (36–39). The wide spectrum antiviral activity suggests a cell-mediated effect rather than a specific viral target. The possibility that maturation of viral glycoproteins may be involved in the antiviral activity against hepatitis B and C viruses is currently under study. In the case of rotavirus, TIZ-induced modification of the structural viral glycoprotein VP7 has been recently shown,<sup>4</sup> reinforcing the hypothesis that maturation and transport of key viral glycoproteins could be a general mechanism of the antiviral activity of this new class of drugs. The finding that thiazolides do not significantly affect the replication of human rhinovirus, a picornavirus whose maturation does not require viral glycoprotein trafficking to the cell membrane, further supports this hypothesis.

In the case of influenza viruses, targeting the maturation of the viral hemagglutinin, a key step for correct assembly and exit of the virus from the host cell, offers the opportunity to disrupt the production of infectious viral particles attacking the pathogen at a level different from the currently available anti-influenza drugs. NTZ is a licensed product in the United States for the treatment of infectious gastroenteritis and is undergoing phase II clinical trials in the United States and abroad in the treatment of chronic hepatitis C (36, 39). The drug has been shown to be safe and effective even when given over a year, and

phase II clinical studies could be initiated in the treatment of influenza at any time in the future. Clinical trials have recently demonstrated activity of commercially available pharmaceutical formulations of NTZ in treating rotavirus gastroenteritis (36) and chronic hepatitis B and C (38, 39). If anti-influenza activity can be established in humans, NTZ could provide a much needed addition to the armamentarium of drugs used for chemoprophylaxis and treatment of influenza.

*Acknowledgments*—We are grateful to Dr. Enrique Rodriguez-Boulan (Cornell University, New York, NY) for anti-PR8 polyclonal antibodies and LDLR-A18-GFP plasmid and Dr. Isabella Donatelli (Istituto Superiore di Sanità, Rome, Italy) for providing the A/Firenze/7/03, A/Ck/It/9097/97 and B/Parma/3/04 influenza viruses. We also thank Drs. Stefania Carta and Carla Amici for help in the characterization and production of A/Ck virus and Palma Mattioli for assistance with the DeltaVision Imaging system.

## REFERENCES

1. Fiore, A. E., Shay, D. K., Broder, K., Iskander, J. K., Uyeki, T. M., Mootrey, G., Bresee, J. S., and Cox, N. S. (2008) *MMWR Recomm. Rep.* **57**, 1–60
2. Wright, P. F., Neumann, G., and Kawaoka, Y. (2007) in *Field's Virology*, 5th Ed., pp. 1691–1740, Lippincott, Williams and Wilkins, Philadelphia
3. Palese, P., and Shaw, M. (2007) in *Field's Virology*, 5th Ed., pp. 1647–1689, Lippincott, Williams and Wilkins, Philadelphia
4. Cox, N. J., and Subbarao, K. (1999) *Lancet* **354**, 1277–1282
5. Gu, J., Xie, Z., Gao, Z., Liu, J., Korteweg, C., Ye, J., Lau, L. T., Lu, J., Gao, Z., Zhang, B., McNutt, M. A., Lu, M., Anderson, V. M., Gong, E., Yu, A. C., and Lipkin, W. I. (2007) *Lancet* **370**, 1137–1145
6. Hayden, F. G., Fritz, R., Lobo, M. C., Alvord, W., Strober, W., and Straus, S. E. (1998) *J. Clin. Invest.* **101**, 643–649
7. Cheung, C. Y., Poon, L. L., Lau, A. S., Luk, W., Lau, Y. L., Shortridge, K. F., Gordon, S., Guan, Y., and Peiris, J. S. (2002) *Lancet* **360**, 1831–1837
8. Bernasconi, D., Amici, C., La Frazia, S., Ianaro, A., and Santoro, M. G. (2005) *J. Biol. Chem.* **280**, 24127–24134
9. Ghedin, E., Sengamalai, N. A., Shumway, M., Zaborsky, J., Feldblyum, T., Subbu, V., Spiro, D. J., Sitz, J., Koo, H., Bolotov, P., Dernovoy, D., Tatusova, T., Bao, Y., St George, K., Taylor, J., Lipman, D. J., Fraser, C. M., Taubenberger, J. K., and Salzberg, S. L. (2005) *Nature* **437**, 1162–1166
10. Webby, R. J., and Webster, R. G. (2003) *Science* **302**, 1519–1522
11. Horimoto, T., and Kawaoka, Y. (2005) *Nat. Rev. Microbiol.* **3**, 591–600
12. Fox, L. M., and Saravolatz, L. D. (2005) *Clin. Infect. Dis.* **40**, 1173–1180
13. Rossignol, J. F., Kabil, S. M., El-Gohary, Y., and Younis, A. M. (2006) *Clin. Gastroenterol. Hepatol.* **4**, 320–324
14. Rossignol, J. F., Ayoub, A., and Ayers, M. S. (2001) *J. Infect. Dis.* **184**, 381–384
15. La Frazia, S., Amici, C., and Santoro, M. G. (2006) *Antivir. Ther.* **11**, 995–1004
16. Donatelli, I., Campitelli, L., Di Trani, L., Puzelli, S., Selli, L., Fioretti, A., Alexander, D. J., Tollis, M., Krauss, S., and Webster, R. G. (2001) *J. Gen. Virol.* **82**, 623–630
17. Pica, F., Palamara, A. T., Rossi, A., De Marco, A., Amici, C., and Santoro, M. G. (2000) *Antimicrob. Agents Chemother.* **44**, 200–204
18. Rossi, A., Kapahi, P., Natoli, G., Takahashi, T., Chen, Y., Karin, M., and Santoro, M. G. (2000) *Nature* **403**, 103–108
19. Rossi, A., Ciafrè, S., Balsamo, M., Piermarchi, P., and Santoro, M. G. (2006) *Cancer Res.* **66**, 7678–7685
20. Caselli, E., Fiorentini, S., Amici, C., Di Luca, D., Caruso, A., and Santoro, M. G. (2007) *Blood* **109**, 2718–2726
21. Sarge, K. D., Murphy, S. P., and Morimoto, R. I. (1993) *Mol. Cell Biol.* **13**, 1392–1407
22. Glaser, L., Conenello, G., Paulson, J., and Palese, P. (2007) *Virus Res.* **126**, 9–18
23. Sekikawa, K., and Lai, C. J. (1983) *Proc. Natl. Acad. Sci.* **80**, 3563–3567

<sup>4</sup> M. G. Santoro and J. F. Rossignol, unpublished results.

## Thiazolides Inhibit Influenza Virus HA Maturation

24. Mir-Shekari, S. Y., Ashford, D. A., Harvey, D. J., Dwek, R. A., and Schulze, I. T. (1997) *J. Biol. Chem.* **272**, 4027–4036
25. Steinhauer, D. A., and Skehel, J. J. (2002) *Annu. Rev. Genet.* **36**, 305–332
26. Hebert, D. N., Foellmer, B., and Helenius, A. (1995) *Cell* **81**, 425–433
27. Tatu, U., Hammond, C., and Helenius, A. (1995) *EMBO J.* **14**, 1340–1348
28. Ohuchi, R., Ohuchi, M., Garten, W., and Klenk, H. D. (1997) *J. Virol.* **71**, 3719–3725
29. Mishin, V. P., Novikov, D., Hayden, F. G., and Gubareva, L. V. (2005) *J. Virol.* **79**, 12416–12424
30. Subbarao, K., and Joseph, T. (2007) *Nat. Rev. Immunol.* **7**, 267–278
31. Regoes, R. R., and Bonhoeffer, S. (2006) *Science* **312**, 389–391
32. Copeland, C. S., Zimmer, K. P., Wagner, K. R., Healey, G. A., Mellman, I., and Helenius, A. (1988) *Cell* **53**, 197–209
33. Schulze, I. T. (1997) *J. Infect. Dis.* **176**, S24–28
34. Copeland, C. S., Doms, R. W., Bolzau, E. M., Webster, R. G., and Helenius, A. (1986) *J. Cell Biol.* **103**, 1179–1191
35. Jin, H., Leser, G. P., Zhang, J., and Lamb, R. A. (1997) *EMBO J.* **16**, 1236–1247
36. Rossignol, J. F., Abu-Zekry, M., Hussein, A., and Santoro, M. G. (2006) *Lancet* **368**, 124–129
37. Korba, B. E., Montero, A. B., Farrar, K., Gaye, K., Mukerjee, S., Ayers, M. S., and Rossignol, J. F. (2008) *Antivir. Res.* **77**, 56–63
38. Rossignol, J. F., and Keeffe, E. B. (2008) *Future Microbiol.* **3**, 539–545
39. Rossignol, J. F., Elfert, A., El-Gohary, Y., and Keeffe, E. B. (2009) *Gastroenterology* **136**, 856–862
40. Kreitzer, G., Schmoranzner, J., Low, S. H., Li, X., Gan, Y., Weimbs, T., Simon, S. M., and Rodriguez-Boulan, E. (2003) *Nat. Cell Biol.* **5**, 126–136